

# Privacy-Preserving in Connected and Autonomous Vehicles Through Vision to Text Transformation

**Abdolazim Rezaei<sup>1</sup>, Fellow, IEEE, Mehdi Sookhak<sup>2</sup> (Senior Member, IEEE), and Ahmad Patooghy (Senior Member, IEEE)<sup>3</sup>**

<sup>1</sup>Department of Computer Science, Texas A&M University Corpus Christi, Corpus Christi, TX 78412 USA

<sup>2</sup>Department of Computer Science, Texas A&M University Corpus Christi, Corpus Christi, TX 78412 USA

<sup>3</sup>Department of Computer Science, North Carolina A&T State University, Greensboro, NC 27411 USA

Corresponding author: M. Sookhak (email: m.sookhak@ieee.org).

This work was supported in part by the Scholar Achievement in Graduate Education (SAGE) Fellowship Award.

---

**ABSTRACT** Connected and Autonomous Vehicles (CAVs) rely on a range of devices that often process privacy-sensitive data. Among these, roadside units play a critical role particularly through the use of AI-equipped (AIE) cameras for applications such as violation detection. However, the privacy risks associated with captured imagery remain a major concern, as such data can be misused for identity theft, profiling, or unauthorized commercial purposes. While traditional techniques such as face blurring and obfuscation have been applied to mitigate privacy risks, individual privacy remains at risk, as individuals can still be tracked using other features such as their clothing. This paper introduces a novel privacy-preserving framework that leverages feedback-based reinforcement learning (RL) and vision-language models (VLMs) to protect sensitive visual information captured by AIE cameras. The main idea is to convert images into semantically equivalent textual descriptions, ensuring that scene-relevant information is retained while visual privacy is preserved. A hierarchical RL strategy is employed to iteratively refine the generated text, enhancing both semantic accuracy and privacy. Evaluation results demonstrate significant improvements in both privacy protection and textual quality, with the Unique Word Count increasing by approximately 77% and Detail Density by around 50% compared to existing approaches.

**INDEX TERMS** Connected and Autonomous Vehicles, Feedback-based Learning, Privacy, Reinforcement Learning, Vision Language Model

---

## I. INTRODUCTION

PRIVACY in Connected and Autonomous Vehicles (CAVs) has become a major concern in recent years, especially as a growing number of electronic devices are integrated into these vehicles. These systems transfer vehicle data to machine learning (ML)-based image processing pipelines for tasks such as image classification, object detection, face detection and recognition, image enhancement and restoration, and augmented reality. Among these technologies, Artificial Intelligence Equipped (AIE) cameras, which are increasingly deployed at junctions and traffic lights—are now integrated with CAV systems to monitor driver behavior (e.g., mobile phone use and seatbelt compliance) and to capture images for traffic monitoring, violation detection, and safety assessment, all aimed at enhancing public safety.

Despite the financial and operational success of AIE camera systems, their deployment has raised serious privacy

concerns. For example, in Queensland, Australia, an AIE camera initiative has generated approximately \$419.8 million in revenue since 2021 [1], [2], yet civil liberties advocates have objected to the use of these systems due to their potential to capture intimate images of drivers and passengers. As illustrated in Figure 1, the interior of vehicles—widely regarded as a private space—can be inadvertently exposed, raising legal and ethical concerns. Similar issues have been reported in U.S. states such as California and Maryland, where AIE cameras have been deployed despite ongoing legal challenges [3]. These deployments underscore broader concerns around visual data privacy in CAVs, which involve not only images but also GPS data, biometric identifiers, and audio streams [4].

According to recent studies [4], [5], compromising the privacy of such data can result in consequences such as identity theft, unauthorized surveillance, user profiling, and

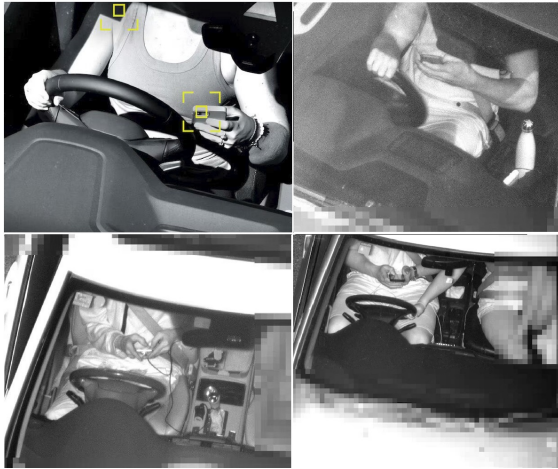


**FIGURE 1.** Sample images captured in the Queensland project where the privacy is not preserved [1], [2].

commercial exploitation. Xie et al. [6] emphasize that the vehicle interior is an extension of personal space and must be protected accordingly. While techniques such as blurring and obfuscation are commonly used to mask sensitive content, they are often inaccurate and may fail to fully conceal private regions. Additionally, recent advances in AI-based reconstruction attacks pose serious threats, enabling adversaries to reverse these privacy measures and reveal the original content.

Given the limitations of existing privacy-preserving techniques, such as inaccurate blurring and vulnerability to AI-based reconstruction attacks, there is a clear need for more robust solutions. In response, this study proposes a novel framework that transforms visual data into descriptive text using advanced VLMs, thereby avoiding the direct exposure of image content.

The core idea of the proposed model is to leverage VLM techniques to generate descriptive text from collected images, capturing all necessary information without revealing the actual visual content. To enhance the quality and relevance of the generated descriptions, we introduce a feedback-based reinforcement learning (RL) framework that operates in parallel with a Retrieval-Augmented Generation (RAG) mechanism. RAG plays a key role in optimizing prompt selection by double-checking and refining the prompts used during RL training. To the best of our knowledge, this is the first attempt to combine RL and VLM for transforming visual data into text as a means of privacy preservation.

The core contributions of this study are as follows:

- 1) Development of an iterative image-to-text transformation architecture, which generates semantically rich and privacy-aware descriptive text from visual data.
- 2) Design of a hierarchical RL mechanism that refines both prompts and generated outputs in multiple stages.
- 3) Integration of a feedback-based learning loop using RAG to validate and optimize prompt selection, thereby improving the relevance and accuracy of the generated text.

**TABLE 1.** List of acronyms used in this article.

Acronym	Expression
CAV(s)	Connected and Autonomous Vehicle(s)
RL	Reinforcement Learning
VLM(s)	Vision Language Model(s)
DP	Differential Privacy
FL	Federated Learning
IoT	Internet of Things
PPO	Proximal Policy Optimization
SBERT	Sentence-BERT
RAG	Retrieval Augmented Generation
MSE	Mean Squared Error
SSIM	Structural Similarity Index Measure
LLM	Large Language Model
AIE	AI-Equipped
MIPS	Maximum Inner Product Search

The rest of this paper is organized as follows. Related Work reviews the existing literature and background methods. Proposed Model introduces the RL-VLM framework. Results and Discussions describes the experimental setup and presents the results. Finally, Conclusion and Future Work summarizes the key findings and outlines directions for future research.

A list of acronyms used in this article is provided in Table 1.

## II. RELATED WORK

Privacy in the context of CAVs is a complex term with multiple implications. For example, the authors in [7] focus on counting passengers at bus station without showing their faces. In [8], the goal is to collect traffic data while protecting individuals' privacy. Another study by Zhang et al. [9] looks inside the vehicle to count passengers, also considering privacy concerns. Therefore, it can be said that the definition of privacy can vary based on the situation.

There have been many privacy preservation studies where researchers have proposed different ways to manipulate parts of the target image. For example, in [10], the authors propose a face masking method to issue tickets. In another study [11] the authors focus on image obfuscation to protect privacy. Face obfuscation, masking, fogging, and replacements are the most common methods to avoid compromising privacy of images [12], [13]. However, existing methods are not capable to ensure privacy preservation. For example, Jian et al. in [14] explain how these methods are likely vulnerable to some AI methods such as adversarial attacks where attackers can recover identities. In a similar study [15], the author discusses the vulnerability of visual information hiding methods that are susceptible to adversarial attacks. In the Queensland case [1], [2], the goal was to detect driving violations, but parts of the driver's body were still visible even though partial fogging is applied, and this raises additional privacy concerns. In a similar case, The State

of Maryland uses AIE roadside cameras to detect traffic violations [3]. These cameras try to blur the driver's face, but this does not fully guarantee visual privacy. In fact, a major problem with these methods is that they may incorrectly target parts of the image that involve privacy concerns [6], [16].

### III. PROPOSED SOLUTION

This section presents the proposed hierarchical framework, which integrates VLM, RL, and RAG to address image privacy challenges in CAVs. Visual data is first captured by AIE cameras and transformed into textual descriptions using a VLM, which generates responses based on selected prompts aimed at minimizing exposure of sensitive content. A feedback-driven RL agent is employed to iteratively refine the prompt selection process. However, since the VLM's prompt selection may not always yield optimal results, a RAG module is incorporated to monitor performance and enhance overall system effectiveness by retrieving and integrating relevant contextual information. The main components and operational flow of the proposed framework are detailed in the following four steps.

#### Step 1: VLM for Text Generation

At the heart of the model is a VLM model that converts images into textual descriptions. This component is particularly effective due to its dual-modality architecture, which enables the model to learn joint representations of visual and linguistic information, as illustrated in Figure 2. The VLM first performs object extraction with high accuracy, guided by the following loss function:

$$Loss = \sum_{i=0}^{s^2} \sum_{c \in classes} 1_{obj}^{ij} (p_i(c) - \hat{p}_i(c))^2$$

where  $1_{obj}^i$  indicates whether an object exists in cell  $i$ ,  $p_i$  is the true class probability distribution for cell  $i$ , and  $\hat{p}_i$  is the predicted distribution.

The VLM generates descriptions by matching images with textual prompts, allowing it to produce rich summaries of visual content. These textual prompts are not arbitrary but rather follow a hierarchical structured list of predefined prompts that guide the model in extracting key visual elements, such as vehicles, pedestrians, or existing conditions within the image. This ensures that the descriptions are relevant and actionable for further processing. By encoding complex images into text, this step compresses the data while maintaining the semantic information necessary for an accurate representation in the cloud environment.

Initially the model starts with token embedding  $X = [x_1, x_2, \dots, x_n]$ ,  $x_i \in \mathbb{R}^d$  where  $X$  is the input matrix of token vectors,  $n$  is the length of the sequence, and  $d$  is the embedding dimension. Positional encoding are added to represent token positions in a sequence because through the following equation since Transformers do not have a built-in notion of

sequence order:  $PE(pos, 2i) = \sin(\frac{pos}{10000^{\frac{2i}{d}}})$ ,  $PE(pos, 2i + 1) = \cos(\frac{pos}{10000^{\frac{2i+1}{d}}})$

The positional embedding vector is added to the token embedding:  $Z_0 = X + P$  where  $P$  represents the positional encoding. The weighted combinations of the token embeddings for each layer including input vectors are linearly transformed into  $Query(Q)$ ,  $Key(K)$ , and  $Value(V)$  matrices using learnable weight matrices  $W^Q$ ,  $W^K$ , and  $W^V$ . The core of the attention mechanism is the scaled dot-product attention, which computes attention scores for each pair of tokens through:  $Attention(Q, K, V) = \text{Softmax}(\frac{QK^T}{\sqrt{d_k}})V$  where  $QK^T$  computed the dot-product similarity between queries and keys. The term  $\frac{1}{\sqrt{d_k}}$  scales the dot product to prevent extremely large values, which could lead to small gradients. Also, the softmax normalizes these scores across all tokens, generating a probability distribution to determine the importance of each token. Then the self-attention mechanism is repeated multiple times in multi-head attention to learn different aspects of the input sequence:  $MultiHead(Q, K, V) = \text{Concat}(\text{head}_1, \text{head}_2, \dots, \text{head}_h)W^O$  where each head is calculated using sets of weights, and  $W^O$  is a weight matrix to linearly project the concatenated heads. After the attention mechanism, each token's representation passes through a feed-forward network. This is done for each token independently, which consists of two linear transformations with a non-linear ReLU activation function:  $FFN(z) = \text{ReLU}(zW_1 + b_1)W_2 + b_2$  where  $W_1, W_2$  are weight matrices, and  $b_1, b_2$  are biases. To stabilize training, Layer Normalization and Residual Connections are used. In the first one each sub-layer (multi-head attention and FFN) has a skip connection that bypasses the layer and adds its input directly to the output.  $Z_i = \text{LayerNorm}(Z_i + \text{SubLayer}(Z_i))$  The Layer Normalization normalizes the inputs to stabilize and accelerate training, typically computed as:  $\text{LayerNorm}(z) = \frac{z - \mu}{\sigma + \epsilon}$  where  $\mu$  and  $\sigma$  are the mean and standard deviation of the layer activations.

The final output is generated using the softmax function to convert scores into a probability distribution over the vocabulary. This is computed for each token to predict the next token in the sequence:  $P(word_i) = \text{Softmax}(z_L W^V)$  where  $W^V$  is the learned weight matrix that projects the final token embeddings into vocabulary size. To train the model, backpropagation is used to update the weights to minimize the loss. The key calculations here include cross-entropy Loss function and a gradient descent optimization through the following equations:  $L = -\sum_{i=1}^{N-1} y_i \log(\hat{y}_i)$  and  $\theta_{t+1} = \theta_t - \alpha \frac{m_t}{\sqrt{v_t + \epsilon}}$  where  $m_{t+1}$  and  $V_t$  are estimates of the first and second moments of the gradients, and  $\alpha$  is the learning rate.

#### Step 2: Prompt Selection Using RL

In this step, initial textual descriptions generated by the VLM are refined using the proposed RL model. The RL model optimizes the text by mapping it to the most relevant and specific prompts from a refined list. This process en-

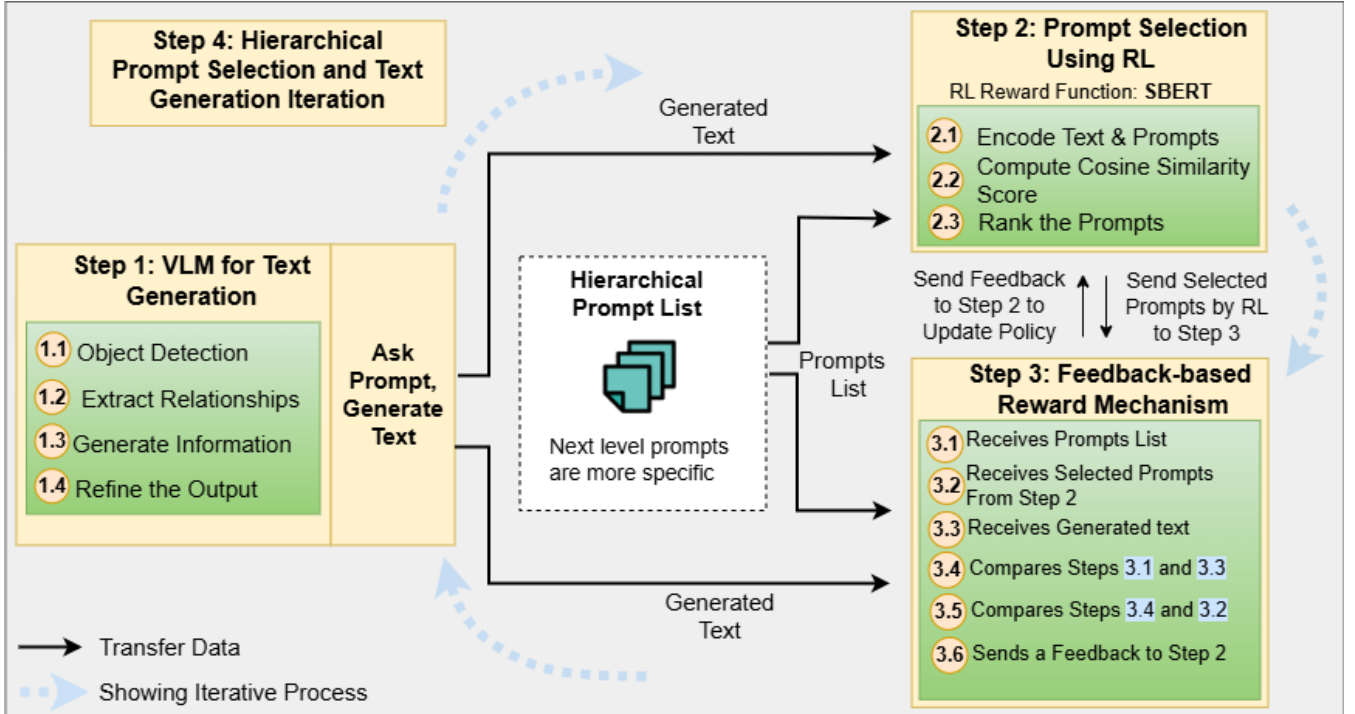


FIGURE 2. Feedback-based RL-VLM model.

hances both relevance and specificity, resulting in concise yet context-aware descriptions that align with the requirements of the target digital environment.

The RL model enhances hierarchical text generation by dynamically refining text based on training feedback, improving precision. It adjusts general descriptions by selecting prompts that highlight specific image details such as vehicles in traffic or industrial objects. Proximal Policy Optimization (PPO), a widely adopted RL method across various domains [17], is employed in this study to achieve the desired performance. The policy objective function for PPO is computed through the probability ratio:

$$r_\theta = \frac{\pi_\theta(a_t|s_t)}{\pi_{\theta_{old}}(a_t|s_t)}$$

where  $r_\theta$  is the *reward value*,  $\pi_\theta$  is new *policy*,  $a_t$  is the *action*, and  $s_t$  is *observation space*. The objective function is based on the **advantage function**,  $A_t$ , which estimates how much a new action is better than its older counterpart through the following expected reward:

$$L_t(\theta) = \mathbb{E}[r_t(\theta)A_t].$$

Considering PPO policy, the extended equation would be

$$L^{PPO}(\theta) = \mathbb{E}[\min(r_\theta A_t, \text{clip}(r_\theta, 1 - \epsilon, 1 + \epsilon)A_t)]$$

which is comprised of  $r_\theta = \frac{\pi_\theta(a_t|s_t)}{\pi_{\theta_{old}}(a_t|s_t)}$  as probability ratio, and  $A_t$  as the advantage function  $A_t = Q(s_t, a_t) - V(s_t)$ .

Considering all components, we get:

$$L^{PPO}(\theta) = \mathbb{E}[\min\left(\frac{\pi_\theta(a_t|s_t)}{\pi_{\theta_{old}}(a_t|s_t)}\right) \cdot A_t, \text{clip}\left(\frac{\pi_\theta(a_t|s_t)}{\pi_{\theta_{old}}(a_t|s_t)}, 1 - \epsilon, 1 + \epsilon\right) \cdot A_t]$$

If the new policy, controlled by  $\epsilon$ , improves the performance within a trust region then it updates normally. If the improvement is too large, the function prevents it from overshooting to avoid instability. This ensures stable learning and limits how much the new policy deviates from the old one per an update.

As illustrated in Figure 2, after generating the refined text, a reward function is integrated into the core of the RL model. A pre-trained SBERT model [18] is employed to score and rank the refined prompts based on their semantic similarity to the input text. SBERT, a state-of-the-art model for generating sentence embeddings, enables efficient calculating of semantic similarity between textual elements. In this process, SBERT encodes both the generated text and the refined list of prompts. Cosine similarity scores are then calculated between the text and each prompt. This similarity score represents how well the prompt aligns with the input text. Prompts are ranked based on these scores, allowing the model to filter out irrelevant or redundant information and pass only the most relevant prompts to the next stage.

### Step 3: Feedback-Based Reward Mechanism

Despite the successful extraction of the relative text from the images, the efficiency of the proposed model can be improved by adding an external function. The main idea is

**Algorithm 1** The Proposed Algorithm with Feedback Mechanism

**Require:**

```

1: iteration  $\geq 1$ 
Ensure: Policy is updated and refined prompts generated
2:  $i \leftarrow 1$ 
3: iteration  $\leftarrow 3$ 
4: feedback  $\leftarrow \text{False}$ 
5: PU  $\leftarrow \text{None}$ 
6: while  $i \leq \text{iteration}$  do:
7:   ObjectDetection()
8:   if feedback then
9:     UpdatePolicy(PU)
10:    feedback  $\leftarrow \text{False}$ 
11:   end if
12:   ComputeSimilarityScore()
13:   PromptSelection()
14:   ComputeReward()
15:   EvaluationAndSelection(Text, Prompt List)
16:   UpdatePromptList()
17:   Compute  $\mathcal{L}(\theta)$ 
18:    $s \leftarrow \text{EvaluateSimilarity}(): \text{armaxSim}(q, D_i)$ 
19:   PU  $\leftarrow \text{PolicyUpdates}(s)$ 
20:   if PU then:
21:     feedback  $\leftarrow \text{True}$ 
22:   end if
23:    $i \leftarrow i + 1$ 
24: end while

```

to propose a feedback-based RL framework to validate the process after extracting the refined text. To achieve this goal, RAG [19] employed as an external knowledge augmentation mechanism to evaluate the model performance based on the generated feedback. Integration RAG into the RL agent enables the proposed model to not only provide context-rich feedback but also improve the prompt management process, thereby improving the accuracy of the text refinement.

RAG offers advantages over PPO by dynamically retrieving the most relevant prompts, ensuring contextual accuracy without the need for retraining. In contrast, PPO relies solely on RL and may struggle with new or evolving data. Moreover, RAG is inherently more scalable and can efficiently operate over large knowledge bases.

To improve the accuracy of the generated text, the RAG model analyzes both the generated output and target prompts to identify the most relevant matches. This process occurs in parallel with the operation of the RL model. Once the RL agent selects the most relevant prompts, the RAG output is used to evaluate and validate the results. This stage is designed to correct potential errors or deficiencies in the RL model's output, thereby supporting improved convergence and overall performance.

The feedback-based process creates a loop where the model iteratively improves its text generation by learning

from these evaluations, enabling it to produce highly relevant and precise descriptions. The feedback mechanism operates based on the following equation:

$$L(\theta) = E[r_t(\theta)A_t + \lambda.F(s_t, a_t)]$$

where  $F(s, a)$  represents an external feedback function, and  $\lambda$  is a weighting coefficient that determines the influence of the feedback on the learning process.

In this context, the term  $r_t(\theta)$  denotes the importance sampling ratio, given by  $r_t(\theta) = \frac{\pi_\theta(a_t|s_t)}{\pi_{\theta_{old}}(a_t|s_t)}$ . This ratio adjusts for the difference between the new and old policies. The advantage function,  $A_t$ , is defined as  $A_t = Q(s_t, a_t) - V(s_t)$ , which measures how much better an action  $a_t$  is compared to the expected value under state  $s_t$ . Combining these definitions, the full loss function becomes:

$$L(\theta) = \mathbb{E}_{\approx} \left[ \left( \frac{\pi_\theta(a_t|s_t)}{\pi_{\theta_{old}}(a_t|s_t)} \right) \cdot (Q(s_t, a_t) - V(s_t)) + \lambda.F(s_t, a_t) \right]$$

The augmented RL objective combines the classic policy gradient approach—driven by the advantage term—with knowledge-driven external feedback. Specifically,  $F(s_t, a_t)$  can represent a semantic similarity score, such as one computed by RAG between the generated text and the ground truth. This integration enables the agent to learn not only from environment-based rewards but also from external, domain-specific signals. The hyperparameter  $\lambda$  governs the trade-off between traditional policy learning and feedback correction, allowing flexible adjustment based on the quality and availability of external knowledge. This formulation improves the model's adaptability by integrating corrective feedback alongside environment-driven learning.

The RAG model's evaluation process is based on Maximum Inner Product Search (MIPS), where the most relevant document  $\hat{D}$  is retrieved by computing  $\hat{D} = \text{argmaxSim}(q, D_i)$ , with  $q$  denoting the query embedding generated by the encoder and  $D_i$  representing the embedding of the  $i$ -th document.

#### Step 4: Hierarchical Prompt Selection and Text Generation Iteration

The model uses a hierarchical structure to iteratively improve text descriptions by feeding selective prompts back to the text generator. This loop is repeated three times, progressively enhancing the accuracy and specificity of the descriptions, with a focus on the most important visual details.

By refining the output step by step, the system keeps only the essential information, removing redundant or irrelevant content. This not only reduces the volume of data transmitted to data centers but also ensures that each message precisely captures the corresponding visual scene. The formal definition of the RL model, incorporating its feedback-driven reward component, is outlined below.

**Action Space:** The action space comprises the selection of prompts from a predefined list at each stage. Each action corresponds to an index in the prompt list. For example,

given 10 prompts in List A, the action space is a discrete set  $\{0, 1, \dots, 9\}$ , where each index represents a specific prompt. **Observation Space:** The observation space includes the current state of the generated text and any possible features extracted from it, such as embeddings generated by a language model.

**Reward Set:** The first reward is based on the relevance of the selected prompts to the currently generated text.

**Feedback-Reward Set:** The second reward is a feedback-based reward derived from RAG. As RAG often performs better assessments than the RL model's internal reward signal, its output is used to perform an additional policy update.

**Transition Set:** The transition set consists of tuples  $(s, a, r, s')$  representing the interactions between states, actions, rewards, and resulting states.

Algorithm 1 outlines steps 1-4, demonstrating how the model begins with a base policy and iteratively improves it over three iterations. In each iteration, the policy is first updated based on similarity scores, followed by a second update driven by the computed loss function  $L(\theta)$ , applied when the change leads to measurable performance gains.

## IV. RESULTS AND DISCUSSIONS

The experimental framework is implemented in Python 3.11, where input images are processed to generate descriptive text outputs. To evaluate the generalizability of the proposed model, two datasets are employed: Drive&Act [20], which contains approximately 9.6 million images, and a public traffic-scene dataset from Kaggle [21]. These datasets cover diverse environments to assess the model's performance under varying conditions. Initially the model will be compared with the results obtained from a PPO-based RL model then it will be compared to the model introduced in [22]. Therefore, we also consider CFP-FP and AgeDB-30 datasets to apply.

The evaluation process involves two main categories of metrics: privacy preservation and text quality.

TABLE 2. Privacy Metrics Evaluation on the CFP-FP Dataset

Method	SSIM ↓	PSNR ↓	MSE ↓	SRRA (%) ↓
AdvFace	0.89	23.54	314.7	13.01
PPO-based RL	0.86	23.02	333.7	12.5
Feedback-based (Ours)	<b>0.85</b>	<b>22.18</b>	<b>365.2</b>	<b>11.25</b>

TABLE 3. Privacy Metrics Evaluation on the AgeDB-30 Dataset

Method	SSIM ↓	PSNR ↓	MSE ↓	SRRA (%) ↓
AdvFace	0.87	22.91	347.8	14.12
PPO-based	0.86	21.98	355.5	13.03
Feedback-based (Ours)	<b>0.83</b>	<b>21.88</b>	<b>389.1</b>	<b>12.63</b>

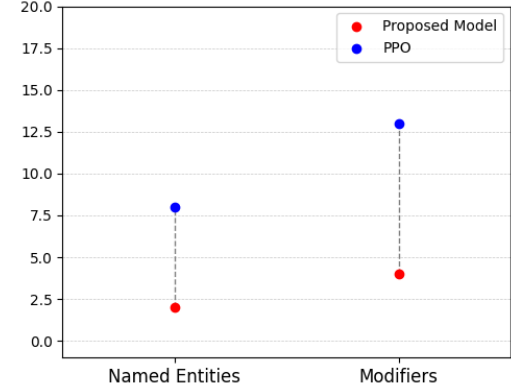


FIGURE 3. NER and Modifiers Metrics.

### A. Privacy Preservation Metrics

To check how well privacy is protected, we use a test called the *Adversarial Reconstruction Test*. In this test, pictures are reconstructed and then compared against the original pictures. The following metrics are used where Table 2 and 3 presents results for the first four metrics, metrics in 5 are shown in Figure 3:

- 1) SSIM evaluates how similar two images are.
- 2) PSNR metric evaluates the quality of a compressed or reconstructed image by calculating the ratio between the maximum possible signal power and the power of the corrupting noise.
- 3) MSE calculates how much each pixel in the reconstructed image differs from the corresponding pixel in the original image.
- 4) SRRA to measure the performance of the protected features.
- 5) Named Entities and Modifiers evaluates whether the model correctly captures specific entities (e.g., people, places, objects) and uses rich descriptive modifiers. As illustrated in Figure 3, the baseline model often leaves such elements, while the proposed model consistently considers more.

### B. Text Quality and Semantic Richness Metrics

The information and linguistic quality of the generated text is assessed by using the following literal and meaning metrics:

- Word Count and Unique Word Count: reflect the length and literal variety of the output. As shown in Figure 4, the proposed model produces a longer and more detailed description than the baseline, and quantitatively indicates better expression.
- Detailed Density: determines the amount of specific and descriptive information relative to the overall length of the text. It captures semantic prosperity by identifying constructions such as subordinate sections and detailed comments. Figure 5 highlights the proposed model produces intensive and more informative details, contributing to more accurate visual understanding.

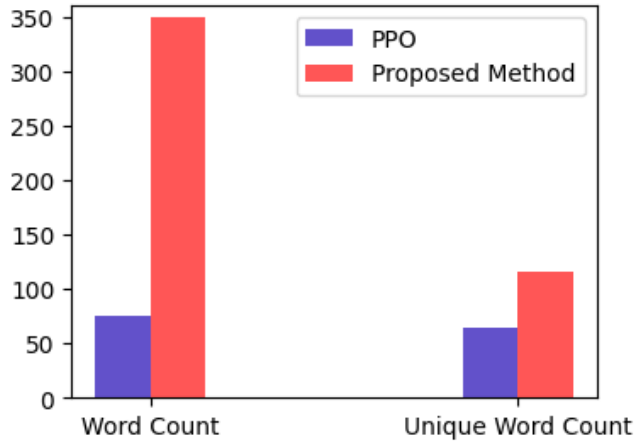


FIGURE 4. Lexical Richness metrics count the number of words.

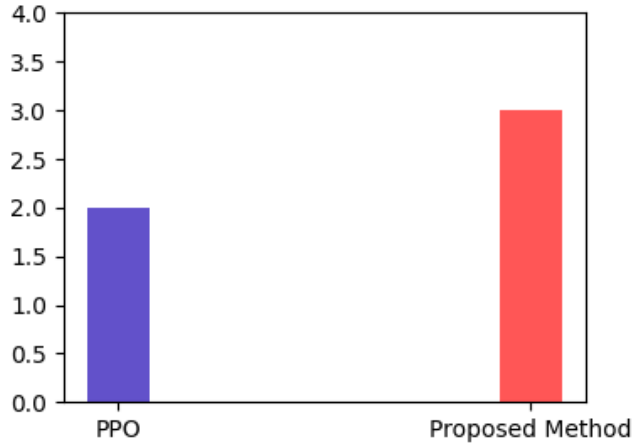


FIGURE 5. Detailed Density is the amount of information per length.

- Semantic Similarity Score: compares two texts generated from the same image to assess the semantic similarity. The score of 0.7371 was obtained, confirming that the proposed model has high meaning alignment with baseline offering richer descriptive text.

Figure 6 illustrates the semantic similarity between the text generated by the baseline model and the proposed model. Initially, the proposed model produces descriptions that are closely aligned with those of the baseline. However, as training progresses, the model receives updates and improvements. After 500 iterations, it reaches a stability, with the baseline model's output remaining approximately 73% semantically similar to the text generated by the proposed model. This demonstrates that the proposed model is capable of enriching the generated text with additional semantic content.

## V. CONCLUSION AND FUTURE WORK

This study introduces a privacy-preserving framework for CAVs leveraging VLMs and RL. The proposed framework

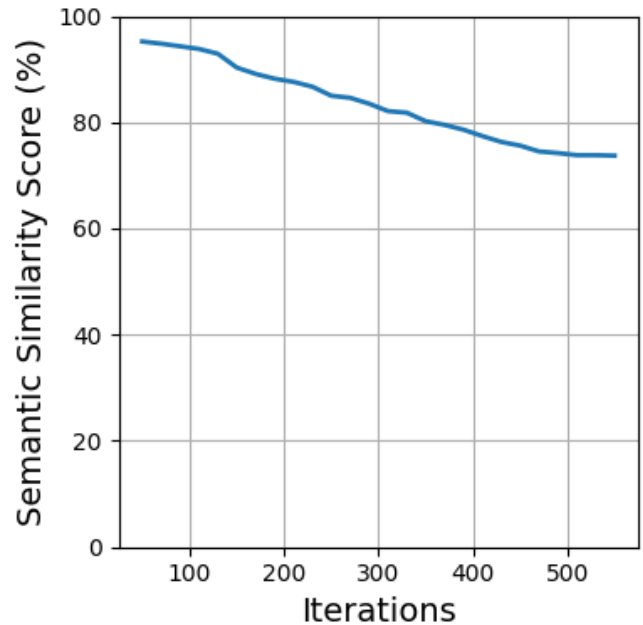


FIGURE 6. Semantic Similarity Score, which indicates how similar the text generated by the baseline method is similar to that of the proposed one.

transforms visual data into concise, semantically rich text with the aim of preserving the individual privacy in the captured images. It demonstrates improved scalability, accuracy, and privacy protection, making it suitable for deployment in smart city infrastructures and industrial automation environments. Evaluations done both on privacy-related and text quality metrics confirm the effectiveness of the proposed method. Although the generated text captures key elements of the image, it excludes sensitive visual details, thereby preserving user privacy. The method can produce three to four times more descriptive content compared to baseline models, without compromising privacy. For future work, we propose exploring dynamic prompt generation, where the prompt list is adaptively updated at each iteration based on context or feedback. This would enable more flexible, personalized, and privacy-aware text generation, further enhancing the model's generalizability and effectiveness.

## ACKNOWLEDGMENTS

The work of Mehdi Sookhak was supported by the US Department of Transportation (USDOT), under Grant No. 69A3552348332, Tier-1 University Transportation Center (UTC) Transportation Cybersecurity Center for Advanced Research and Education (CYBER-CARE).

## REFERENCES

- [1] A. News, "Call for release of privacy reviews on phone detection and seatbelt cameras," 2024, accessed: 2025-02-27. [Online]. Available: <https://www.abc.net.au/news/2024-08-19/call-for-release-privacy-reviews-phone-detection-seatbelt-camera/104228486>
- [2] —, "Qld police cameras catch drivers using mobile phones and not wearing seatbelts," 2021, accessed: 2025-02-

27. [Online]. Available: <https://www.abc.net.au/news/2021-07-08/qld-police-cameras-catch-drivers-mobile-phones-seatbelts/100277298>

[3] T. Sun. (2024) New traffic cameras automatically blur drivers' faces — but issue ai-powered tickets anyway. Accessed: 2025-04-30. [Online]. Available: <https://www.the-sun.com/motors/13632696/new-traffic-cameras-automatically-blur-drivers-faces/>

[4] F. Liu, D. Wang, and Z. Xu, "Privacy-preserving travel time prediction with uncertainty using gps trace data," *IEEE transactions on mobile computing*, vol. 22, no. 1, pp. 417–428, 2021.

[5] S. Boovaraghavan, H. Zhou, M. Goel, and Y. Agarwal, "Kirigami: Lightweight speech filtering for privacy-preserving activity recognition using audio," *Proceedings of the ACM on Interactive, Mobile, Wearable and Ubiquitous Technologies*, vol. 8, no. 1, pp. 1–28, 2024.

[6] C. Xie, Z. Cao, Y. Long, D. Yang, D. Zhao, and B. Li, "Privacy of autonomous vehicles: Risks, protection methods, and future directions," *arXiv preprint arXiv:2209.04022*, 2022.

[7] P. Ghazianni, K. Bajaj, N. Bouguila, and Z. Patterson, "A privacy-preserving edge computing solution for real-time passenger counting at bus stops using overhead fisheye camera," in *2024 IEEE 18th International Conference on Semantic Computing (ICSC)*. IEEE, 2024, pp. 25–32.

[8] X. He, L. Li, H. Peng, and F. Tong, "A multi-level privacy-preserving scheme for extracting traffic images," *Signal Processing*, vol. 220, p. 109445, 2024.

[9] X. Zhang, H. Zhang, K. Li, and Q. Wen, "Privacy-preserving public route planning based on passenger capacity," *Mathematics*, vol. 11, no. 6, p. 1546, 2023.

[10] The U.S. Sun. (2025) New traffic cameras automatically blur drivers' faces – but they're still catching record number of motorists. Accessed: 2025-04-24. [Online]. Available: [https://www.the-sun.com/motors/13632696/new-traffic-cameras-automatically-blur-drivers-faces/?utm\\_source=chatgpt.com](https://www.the-sun.com/motors/13632696/new-traffic-cameras-automatically-blur-drivers-faces/?utm_source=chatgpt.com)

[11] A. B. Popescu, I. A. Taca, A. Vizitiu, C. I. Nita, C. Suciu, L. M. Itu, and A. Scafa-Udriste, "Obfuscation algorithm for privacy-preserving deep learning-based medical image analysis," *Applied Sciences*, vol. 12, no. 8, p. 3997, 2022.

[12] L. Laishram, M. Shaheryar, J. T. Lee, and S. K. Jung, "Toward a privacy-preserving face recognition system: A survey of leakages and solutions," *ACM Computing Surveys*, vol. 57, no. 6, pp. 1–38, 2025.

[13] Z. Huang, F. Tang, Y. Zhang, J. Cao, C. Li, S. Tang, J. Li, and T.-Y. Lee, "Identity-preserving face swapping via dual surrogate generative models," *ACM Transactions on Graphics*, vol. 43, no. 5, pp. 1–19, 2024.

[14] B. Jiang, B. Bai, H. Lin, Y. Wang, Y. Guo, and L. Fang, "Dartblur: Privacy preservation with detection artifact suppression," in *Proceedings of the IEEE/CVF Conference on Computer Vision and Pattern Recognition*, 2023, pp. 16 479–16 488.

[15] M. Ye, W. Shen, J. Zhang, Y. Yang, and B. Du, "Securereid: Privacy-preserving anonymization for person re-identification," *IEEE Transactions on Information Forensics and Security*, vol. 19, pp. 2840–2853, 2024.

[16] Z. Xiao, J. Lin, J. Chen, H. Fu, Y. Li, J. Yuan, and Z. Li, "Privacy preservation network with global-aware focal loss for interactive personal visual privacy preservation," *Neurocomputing*, vol. 602, p. 128193, 2024.

[17] J. Xue, S. Zhang, Y. Lu, X. Yan, and Y. Zheng, "Bidirectional obstacle avoidance enhancement-deep deterministic policy gradient: A novel algorithm for mobile-robot path planning in unknown dynamic environments," *Advanced Intelligent Systems*, vol. 6, no. 4, p. 2300444, 2024.

[18] N. Reimers, "Sentence-bert: Sentence embeddings using siamese bert-networks," *arXiv preprint arXiv:1908.10084*, 2019.

[19] S. Bag, A. Gupta, R. Kaushik, and C. Jain, "Rag beyond text: Enhancing image retrieval in rag systems," in *2024 International Conference on Electrical, Computer and Energy Technologies (ICECET)*. IEEE, 2024, pp. 1–6.

[20] M. Martin, A. Roitberg, M. Haurilet, M. Horne, S. Reiß, M. Voit, and R. Stiefelhagen, "Drive and act: A multi-modal dataset for fine-grained driver behavior recognition in autonomous vehicles," in *The IEEE International Conference on Computer Vision (ICCV)*, Oct 2019.

[21] U. Shah Pirzada. (2025) Traffic-net dataset. [Online]. Available: <https://www.kaggle.com/datasets/umairshahpirzada/traffic-net/data>

[22] Z. Wang, H. Wang, S. Jin, W. Zhang, J. Hu, Y. Wang, P. Sun, W. Yuan, K. Liu, and K. Ren, "Privacy-preserving adversarial facial features," in *Proceedings of the IEEE/CVF Conference on Computer Vision and Pattern Recognition*, 2023, pp. 8212–8221.



**ABDOLAZIM REZAEI** (Member, IEEE) holds a Master of Science degree in Software Engineering from the University of Malaya, Malaysia. He is currently pursuing a Ph.D. in Computer Science at Texas A&M University–Corpus Christi, Texas, USA.

He has been awarded the Scholar Achievement in Graduate Education (SAGE) Fellowship for three consecutive years, from 2022 to 2025. His research focuses on the domain of Connected and Autonomous Vehicles (CAVs), employing cutting-edge Artificial Intelligence and Machine Learning models. He has presented his work at international conferences such as the International Conference for Internet Technology and Secured Transactions (ICITST). Currently, he is involved in several research projects, with forthcoming publications expected in reputable journals and conferences.



**MEHDI SOOKHAK** (Senior Member, IEEE) received the Ph.D. degree in computer science from the University of Malaya (UM), Malaysia, in 2015. He contributed as a Research Assistant with the Center for Mobile Cloud Computing Research (C4MCCR), UM. Following this, from 2015 to 2017, he was a Postdoctoral Fellow with the Department of Systems and Computer Engineering, Carleton University, Canada. He is currently an Assistant Professor of computer science with Texas A&M University (TAMU), Corpus Christi, TX, USA, where he leads the Intelligent Edge and Cellular Network Laboratory (IECNL) and the Co-Lead of the Cybersecurity Center for Advanced Research and Education (CYBER-CAR). Before joining TAMU, he was an Assistant Professor with Arizona State University, from 2017 to 2019, and was an Assistant Professor with Illinois State University, from 2019 to 2021.

He possesses an impressive publication record, with over 70 articles to his credit in renowned journals and conferences, such as IEEE ICC, IEEE GLOBECOM, IEEE PIMRC, IEEE TRANSACTIONS ON PARALLEL AND DISTRIBUTED SYSTEMS, IEEE TRANSACTIONS ON VEHICULAR TECHNOLOGY, IEEE TRANSACTIONS ON CONTROL SYSTEMS TECHNOLOGY, IEEE SYSTEMS JOURNAL, ACM Communications, ACM TOSN, and IEEE Communications Magazine. Furthermore, he contributes significantly to the academic community through his editorial roles on the boards of several ISI-indexed journals, including Vehicular Communications, IEEE CEM, and Electronics. He is also serving as a senior member of IEEE Access journal. His dedication to research extends beyond publications, as he serves as the Principal Investigator (PI) for numerous funded projects by organizations, such as NSF, NIH, NIFA, and DOT. His research expertise spans multiple areas, including vehicular networks, wireless sensors and actuators, mobile communication, cloud and edge computing, blockchain technology, and computer security. He has also taken on leadership roles by chairing conferences, such as IEEE COINS and IEEE ICCE.



**AHMAD PATOOGHY** (Senior Member, IEEE) received the Ph.D. degree in computer engineering from the Sharif University of Technology, Tehran, Iran, in 2011. From 2011 to 2017, he was an Assistant Professor with the Iran University of Science and Technology, Tehran. Then, he joined the University of Central Arkansas, Conway, AR, USA, from 2018 to 2021. Since August 2021, he has been with the Department of Computer Systems Technology, North Carolina Agricultural and Technical State University, and leading the Intelligent Cyber-Systems and Architectures Laboratory. He has published

more than 100 peer-reviewed journal articles and conference proceedings. His research interests include the security and reliability of machine learning applications and accelerators, hardware security in the IoT and cyber-physical systems, and hardware design for machine learning acceleration. He is a Senior Member of IEEE Computer Society and a member of ACM. He has been a Reviewer and a PC Member of various IEEE, ACM, Elsevier, and Springer journals and conferences. He has also served as a Panelist for the National Science Foundation for reviewing grant proposals